



MULTIPATH FADING EFFECTS ON UNCODED AND CODED MULTIPLE FREQUENCY SHIFT KEYING PERFORMANCE IN MOBILE WIRELESS COMMUNICATIONS

Dr. Hassan Awheed Jeiad ¹, Dr. Riyadh Jabbar Sudani Al-Bahadili ²

- 1) Lecturer, Computer Engineering Department, University of Technology, Baghdad, Iraq.
- 2) Assistant Prof, Computer Engineering Department, University of Technology, Baghdad, Iraq.

Received 6/11/2017

Accepted 23/4/ 2018

Published 1/7/2019

Abstract: This paper presents an analysis to multipath fading channel effects on the performance of multiple frequency shift keying (MFSK) modulation that used in mobile wireless communications. These effects take account of AWGN, Rayleigh, and Rician multipath fading environments. The analysis also includes the block coding (BC) in error control coding is used in MFSK receivers such as interleaving, Reed Solomon BC, and Alamouti space-time block coding (STBC). The performance analysis of these models is based on bit-error rate (BER) of uncoded and coded MFSK systems when such models operate under multipath fading channels. The simulation results show that an additional enhancement in BER performance and coding gain is gained by adding a space-time block coding to the combination of interleaving and RS coding compared with uncoded MFSK model but at expense of system complexity.

Keywords: mobile wireless communications, digital modulation, multipath fading channel, block coding

تحليل تأثيرات الخفوت متعدد المسارات لأداء نظام القفل المتحول المتعدد الترددات المرمز وغير المرمز في أنظمة الاتصالات اللاسلكية المتنقلة

الخلاصة: يقدم هذا البحث تحليلاً و تقييم لتأثيرات الخفوت متعدد المسارات على أداء نظام القفل المتحول المتعدد الترددات (MFSK) المستخدم في الاتصالات اللاسلكية النقالية. هذه التأثيرات شملت بيئة قنوات مختلفة (AWGN، Rayleigh، Rician). وشمل التحليل أيضاً ترميز الكتلة (block coding) في السيطرة على الأخطاء والتي تستخدم في مستقبلات MFSK مثل interleaving، Reed Solomon BC و Alamouti STBC. وسوف يستند تحليل أداء هذه النماذج على BER لنظام MFSK المرمز وغير المرمز عندما تعمل هذه الأنظمة تحت قنوات الخفوت متعدد المسارات. وتبين نتائج المحاكاة ان تحسن اضافي في اداء معدل الخطا وكسب الترميز تكتسب باضافة ترميز الزمان-المكان الى توليفة التداخل وترميز RS مقارنة بنموذج MFSK غير المرمز ولكن على حساب تعقيد النظام.

1. Introduction

In mobile wireless communication channels, multipath or propagation paths are complaint where the physical objects reflect the transmitted signal. This behavior produces multipath between transmitter and related receiver. These multipath signals can interfere with the desired signal preventing the receiver from detecting the transmitted signal. When a very short pulse is transmitted on a time-varying multipath

*Corresponding Author : hsn.uot@gmail.com

channel, the receiving signal may appear as a train of pulses. Hence, time spread introduced in the signal and time variations in the structure of the channel are the main characteristics of multipath channel. Furthermore, the signal strength could be reduced when multipath signals are out of phase. This behavior of signal strength reduction is named fading, and these multipath signals can be slow and fast fading. Because of multiple signal propagation paths, the actual received signal level is the vector sum of all signals when multiple signals are received. These signals occurrence from any path or angle of arrival. Some signals in multipath aid the direct path while some others subtract it. Essentially, fading is produced by different physical occurrence like reflection, Doppler shift, scattering, and diffraction. Based on the effect of multipath, there is a large-scale fading which the power of received signal fluctuates slowly as a result of signal attenuation found by the geometry of the path. Also, there is a small-scale fading, when the signal transfers over a length in the order of wavelength. This type of fading leads to rapid variation of the phase and amplitude of the signal [1]. In fact, several models can define the small-scale fading which is Rayleigh fading, and Rician fading [2-4]. The Rayleigh fading is mostly produced by multipath reception. It is a statistical model for the effect of a propagation environment on RF signal. Rayleigh fading is most applicable when there is no line of sight between the transmitter and receiver. The Rician fading model is similar to the Rayleigh fading model, except that in Rician fading, a strong dominant component is present. This dominant component is a stationary signal and is commonly known as the line of sight component [5].

In the Rayleigh flat fading channel model, it is assumed that channel makes amplitude in the model of Rayleigh, that varies in time based on the Rayleigh channel distribution whose probability density function (PDF) is described as [6]:

$$f_{rayleigh}(x) = \frac{x}{\sigma^2} \exp\left(-\frac{x^2}{2\sigma^2}\right), \quad x \geq 0 \quad (1)$$

where σ^2 is the variance of the I and Q components (where I is in-phase and Q is quadrature component) and x is a random variable related to the signal amplitude. It is assumed that all signals arrive with different phases have same attenuation.

There are several path components in wireless communications between the transmitter and receiver antennas. Only one is the main path and others are diffused components. In this condition, other components of multipath signal are covered on the main component and the amplitude of resultant signal follows Rician distribution with the ratio between main component and diffused components is called the Rice factor [7-8]. Rician fading comes as a result of Gaussian channel effect and Doppler-shifted, but usually there is a direct line at all times from the transmitter to the receiver antennas. The Rician distribution has PDF defined by [9]:

$$f_{rician}(x) = \frac{x}{\sigma^2} \exp\left(-\frac{(x^2+A^2)}{2\sigma^2}\right) I_0\left(\frac{Ax}{\sigma^2}\right), \quad x \geq 0, A \geq 0 \quad (2)$$

where A is the signal amplitude of the main (dominant) path and $I_0(\cdot)$ is the zero-order modified Bessel function of the first kind.

In this paper, the multipath fading channel effects on the performance of MFSK modulation will be analyzed. These effects take into account the additive white Gaussian noise (AWGN), Rayleigh, and Rician multipath fading environments. The analysis also includes the block coding (BC) in error control coding used in MFSK receivers such as interleaving, Reed Solomon BC, and Alamouti STBC. The performance analysis of these models is based on BER of uncoded and coded MFSK system (coherent and non-coherent types) when such models operate under multipath fading channels.

2. MFSK under AWGN Effect

In MFSK, the frequency of a fixed amplitude carrier signal (f_c) is altered between two or more values by baseband signal $m(t)$, where the transmitted signal is defined by [10]:

$$S_{MFSK}(t) = \sqrt{\frac{2E_b}{T_b}} \cos\left(2\pi\left(f_c + \frac{l}{2mT_b}\right)t\right), \text{ for } l = 1, 2, \dots, M \quad (3)$$

Where T_b is bit interval, E_b is energy per bit, and m is bits per symbol ($\log_2 M$). To keep orthogonality among frequency carriers in coherent receiver, the minimum frequency spacing is $1/2m T_b$. While for non-coherent receiver, the minimum frequency spacing is $1/m T_b$.

In Fact MFSK is not affected by AWGN, since this type of noise affects only on the carrier's signal amplitude but not on the frequency of carrier's signal. The theoretical BER for non-coherent MFSK is given by [1]:

$$BER_{MFSK/AWGN} = \frac{M/2}{M-1} \sum_{i=1}^{M-1} (-1)^{i+1} \binom{M-1}{i} \frac{1}{i+1} e^{-im\left(\frac{E_b}{N_o}\right)/(i+1)} \quad (4)$$

where $\frac{E_b}{N_o}$ is signal to noise ratio (SNR) per bit, and $\binom{M-1}{i} = \frac{(M-1)!}{(M-1-i)!i!}$.

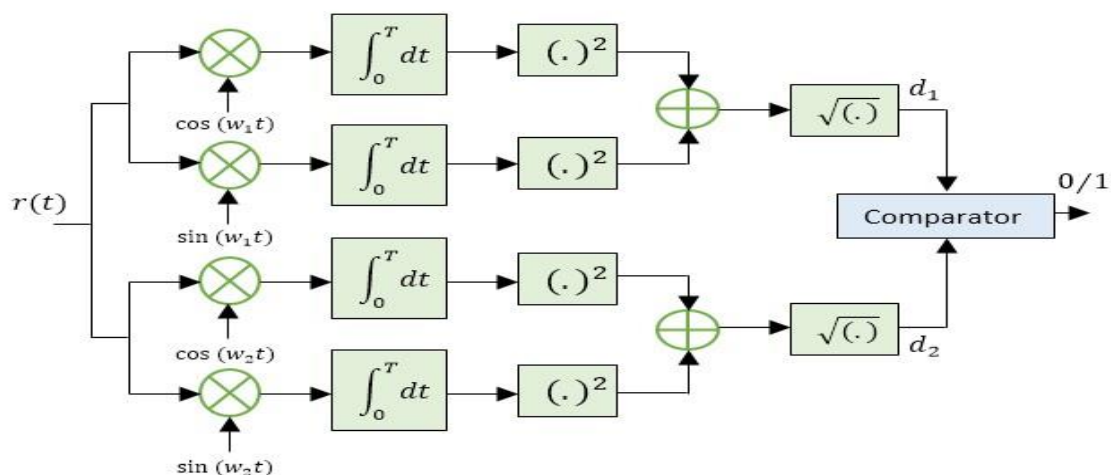


Figure 1. Orthogonal non-coherent 2FSK demodulator [1]

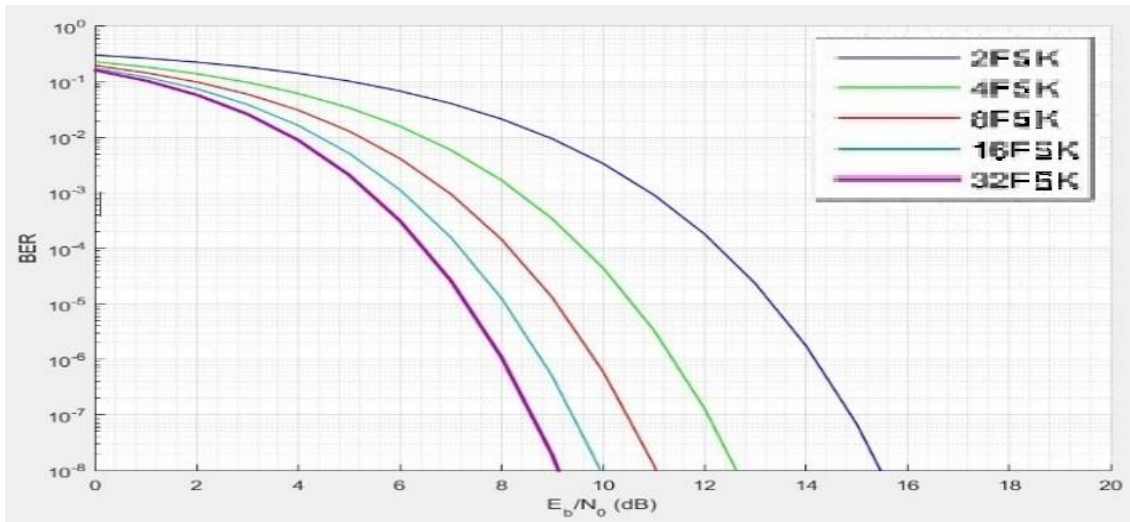


Figure 2. Theoretical BER performance for non-coherent MFSK (M=2, 4, 8, 16, and 32)

Fig.1 shows an orthogonal non-coherent 2FSK modulator that contains two channels (correlators), each one evaluates the correlation between the received signal and two sinusoidal waves at specific frequencies. d_1 and d_2 denotes the envelope samples of the two channels, then if $d_1 > d_2$, symbol 1 is received, otherwise symbol 0 is received. Fig.2 shows the theoretical BER performance for MFSK (M=2, 4, 8, 16, and 32) for non-coherent demodulation under AWGN effect.

3. MFSK under Multipath Fading Effect

In the real environment, the effects of RF propagation are shared and lead to fading channels that produce multipath. Several signals will be received when there is many propagation paths and the resultant received signal is just the sum of incoming signal levels. These incoming signals come from arbitrary angles. Thus, some of reflected signals are in-phase and others are out-phase with the direct path.

The error probability of 2FSK with orthogonal signals in AWGN in the case of non-coherent detection is given by [1]:

$$BER_{2FSK/AWGN} = \frac{1}{2} e^{-\frac{\alpha^2 E_b}{2 N_o}} \quad (5)$$

In the existence of frequency of slow fading, the variable α is Rayleigh-distributed random variable due to receiving multiple paths with no strong component. When averaging error probability (Eq.5) over PDF of $\alpha^2 \frac{E_b}{N_o}$ results:

$$BER_{2FSK/Rayleigh} = \frac{1}{2 + \overline{SNR}_b} \quad (6)$$

where $\overline{SNR}_b = E[\alpha^2] \frac{E_b}{N_o}$ is the average SNR over bit. For $M > 2$, error probability of FSK in Rayleigh fading with non-coherent detection is defined as [1, 15]:

$$BER_{MFSK/Rayleigh} = \frac{M/2}{M-1} \sum_{i=1}^{M-1} (-1)^{i-1} \binom{M-1}{i} \frac{1}{i+1+im\overline{SNR}_b} \quad (7)$$

A Rician channel can be assumed as generalization of Rayleigh channel where a dominant component occurs beside several reflected signals. If the independent Gaussian random variables X_1 and X_2 with variance σ^2 and mean μ , and if α is assumed as distribution random variable for Rician channel, then $\alpha^2 = X_1^2 + X_2^2$ is called non-central Chi squared with two degrees of freedom. The error probability of 2FSK in Rician multipath fading with non-coherent detection is [1, 15]:

$$BER_{2FSK/Rician} = \frac{1+K}{2+2K+\overline{SNR}_b} e^{-\left(\frac{K\overline{SNR}_b}{2+2K+\overline{SNR}_b}\right)} \quad (8)$$

where K is defined as Rice factor and equal to μ^2 / σ^2 .

4. Error Control Coding for MFSK

One way to compensate for BER degradation in MFSK modulation due to channel fading is by using coding process. This paper will analyze the block coding (BC) for error control used in MFSK receivers such as interleaving, Reed Solomon BC [11-13], and Alamouti space-time block coding (STBC) [14]. Reed Solomon BC that will be used in conjunction with MFSK is non-binary, linear cyclic code RS (n, k). For 32FSK, each one of 2^5 symbols is related to one of the $M = 2^5$ orthogonal FSK signals.

To enhance BER performance for MFSK in fading channel, Alamouti STBC 2x2 diversity scheme [15] will be used to give a significant coding gain over uncoded MFSK model.

5. Simulation Results

To estimate the BER performance, Matlab Simulink (R2015a) model implementations have been carried out for MFSK modulation under AWGN and fading environment for uncoded and coded models.

5.1 Uncoded MFSK under AWGN Effect

Fig.3 shows the Simulink model for uncoded MFSK (M=2) with non-coherent detection and under only AWGN effect. The Simulink parameters that used here are as following: M=2, 4, 8, 16, and 32 levels, symbol period and sample time =0.3 sec, frame-based with one sample per frame, frequency spacing=200 Hz and sampling frequency = 10 KHz (3000 samples per symbol).

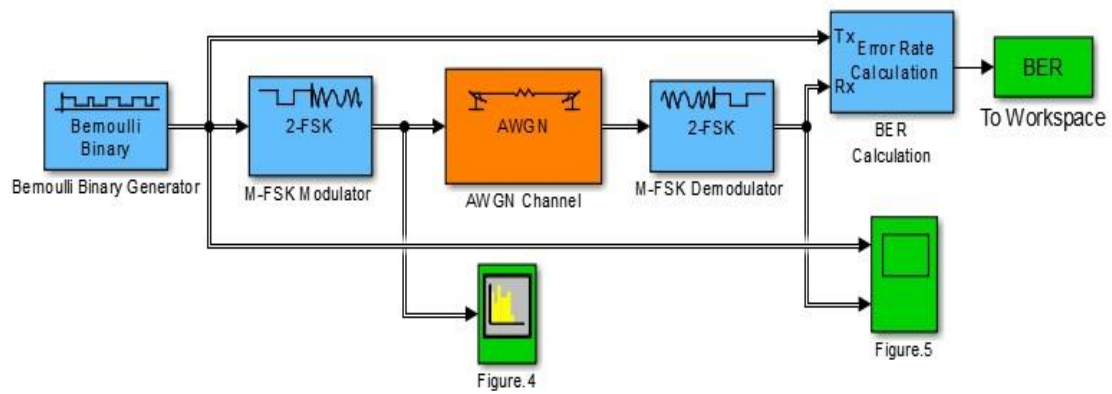


Figure 3. Simulink model for non-coherent uncoded 2FSK detection

The 2FSK margins for each symbol are selected to have continuous phase. Since there are 3000 samples per symbol with 0.3 sec symbol duration, the sampling frequency is 10 KHz greater than Nyquist rate of 200 Hz frequency separation. Fig.4 shows the spectrum of 2FSK modulator using 1024 points FFT with rectangular window. As shown in spectrum, the two frequencies are clearly placed at 100 Hz and -100 Hz. For SNR 10 dB, Fig.5 shows the input of 2FSK modulator and the output of 2FSK demodulator. Clearly, there is no error exists over the time interval at this value of SNR.

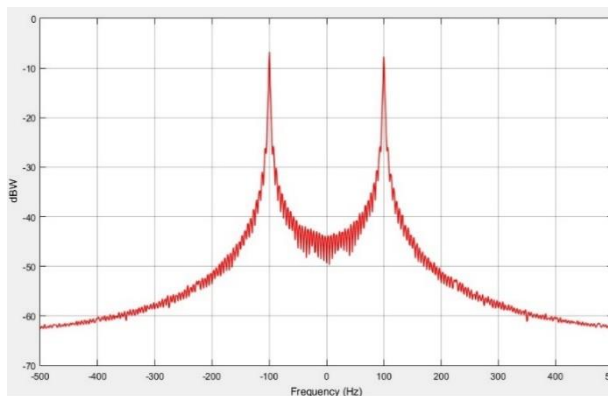


Figure 4. Spectrum of non-coherent 2FSK modulator

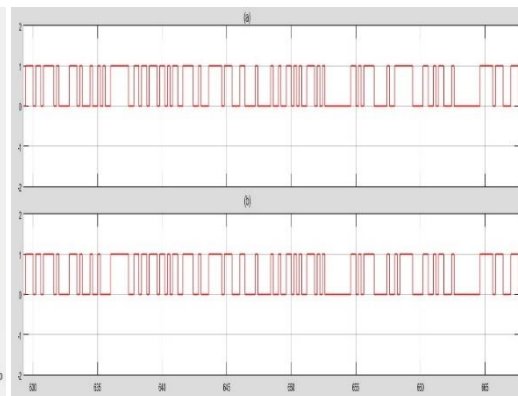


Figure 5. Non-coherent 2FSK at SNR=10 dB (a) modulator input, (b) demodulator output

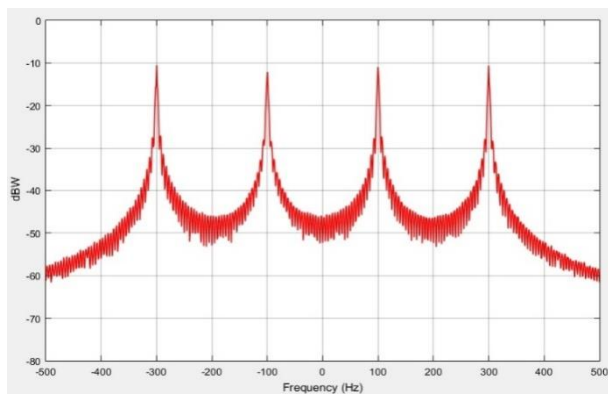


Figure 6. Spectrum of non-coherent 4FSK modulator

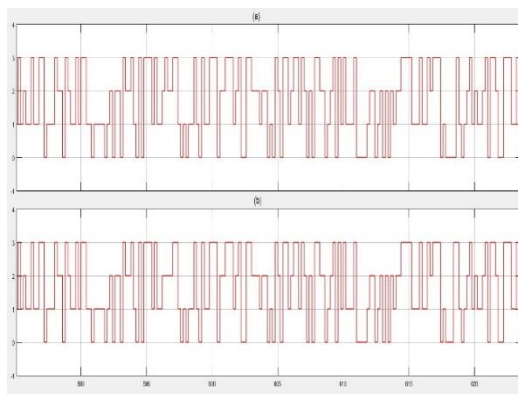


Figure 7. Non-coherent 4FSK at SNR=6 dB (a) modulator input, (b) demodulator output

For 4FSK (gray code mapping), the same model (Fig.3 with M=4) is used to analyze the modulator spectrum and input/output data as shown in Fig.6 and Fig.7.

In Fig.6, there are four frequencies at ∓ 100 and ∓ 300 , while in Fig.7 there is some errors in detection when SNR=6 dB. Fig.8 shows the simulated BER performance of non-coherent MFSK modulation for M=2, 4, 8, 16, and 32 under AWGN effect along with theoretical BER (Eq.4).An acceptable agreement can be shown between the simulated and theoretical values.

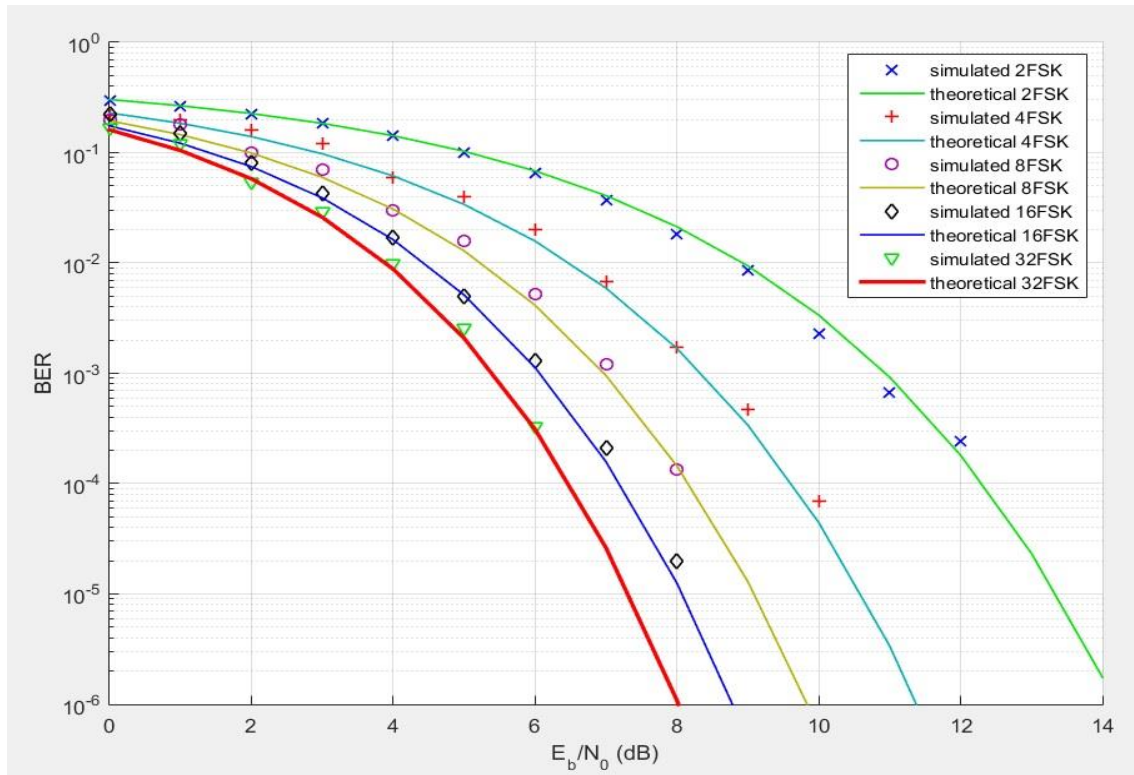


Figure 8. BER performance of non-coherent uncoded MFSK under AWGN effect

5.2 Coded MFSK under AWGN Effect

Reed Solomon BC will be used in conjunction with MFSK is non-binary, linear cyclic code RS (31, 15). $d_{min} = 31 - 15 + 1 = 17$. For 32FSK, each one of 32 symbols is related to one of the $M = 32$ orthogonal FSK signals.

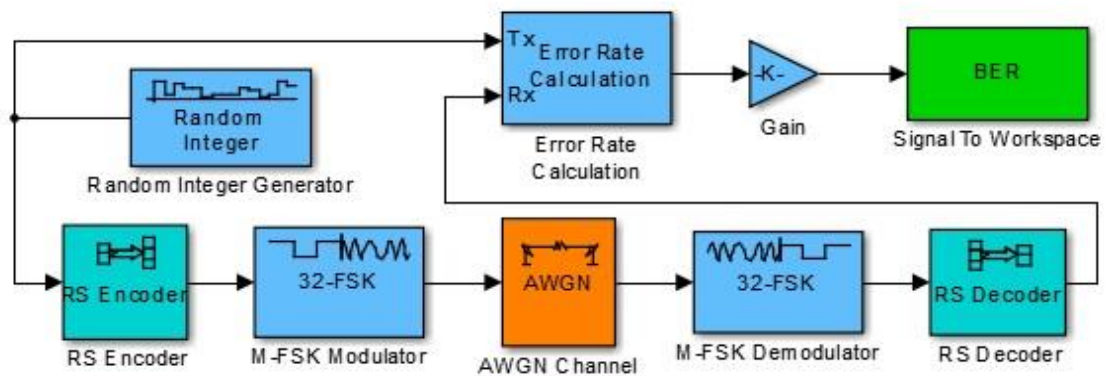


Figure 9. Simulink model for non-coherent coded 32FSK with RS (31,15) under AWGN effect

Fig.9 shows the Simulink model to evaluate BER performance of 32FSK that combined with RS (31, 15) encoder/decoder under AWGN effect. The coded model uses the following parameters: RS symbol time 15/31 sec, frame based with 15 samples per frame, sample period is one sec, the gain of the output is 16/31, hard decisions and non-coherent detection.

The theoretical symbol error rate (SER) for RS (31, 15) with MFSK and non-coherent detection under AWGN is given by [1]:

$$SER_{RS/AWGN} = \frac{1}{n} \sum_{i=t+1}^n i \binom{n}{i} SER_{MFSK}^i (1 - SER_{MFSK})^{n-i} \quad (9)$$

where t is the number of errors the RS (31,15) can correct which is 8 errors, and

$$SER_{MFSK} = \frac{1}{M} \sum_{i=2}^M (-1)^i \binom{M}{i} e^{\left[-\frac{(i-1)mR_c(SNR)}{i}\right]} \quad (10)$$

The equivalent BER is

$$BER_{RS/AWGN} = \frac{M/2}{M-1} SER_{RS/AWGN} \quad (11)$$

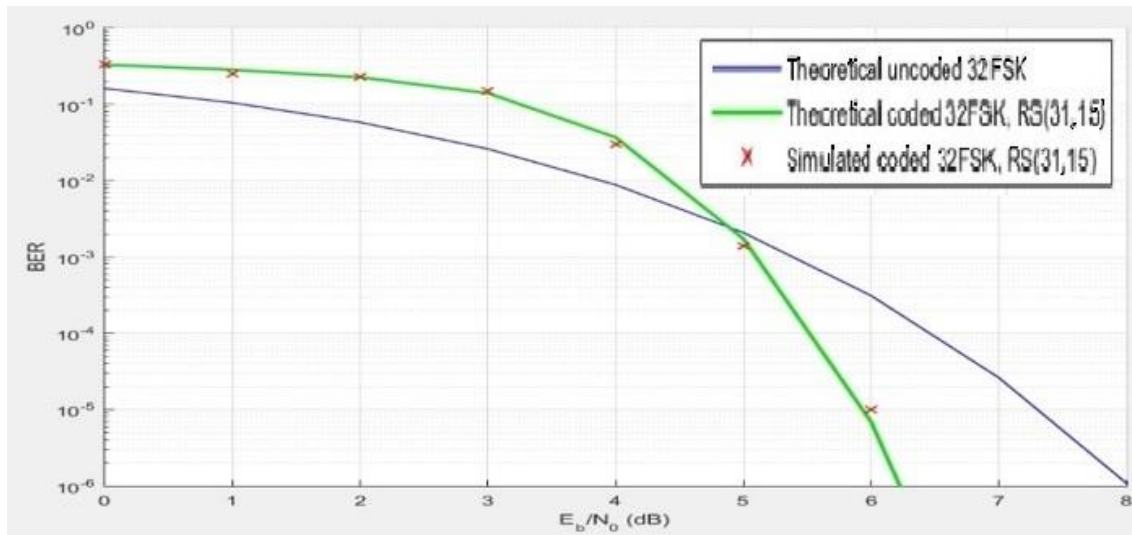


Figure 10. BER performance of non-coherent coded 32FSK with RS (31, 15) under AWGN effect

Fig.10 shows BER performance of non-coherent coded 32FSK with RS (31, 15) under AWGN effect along with uncoded 32FSK performance. An acceptable agreement can be shown between the simulated and theoretical values.

For 32FSK, $BER_{RS/AWGN} = \frac{16}{31} SER_{RS/AWGN}$. Using $M = 32$, $m = 5$, $t = 8$ errors, coding gain $R_c = \frac{15}{31}$, $n = 31$, and $SNR=4$ dB, the theoretical $BER_{RS/AWGN} = 4.13 \times 10^{-2}$ as shown in Fig.10.

5.3 Uncoded MFSK under Multipath Fading Effect

The power spectral density of multipath fading effect characterizes the time-varying channel. This effect is significantly degrading the BER performance of MFSK when goes under fading environment. Fig.11 shows the Simulink model of 2FSK under Rayleigh fading and AWGN channel for the following parameters: symbol time=0.3 sec, 1000 samples per symbol, two frequencies at 100 Hz and -100 Hz, Doppler shift=0.5 Hz. Fig.12 shows the simulated and theoretical BER performance (using eq.6) of non-coherent uncoded 2FSK under Rayleigh fading channel effect along with uncoded 2FSK performance under AWGN alone.

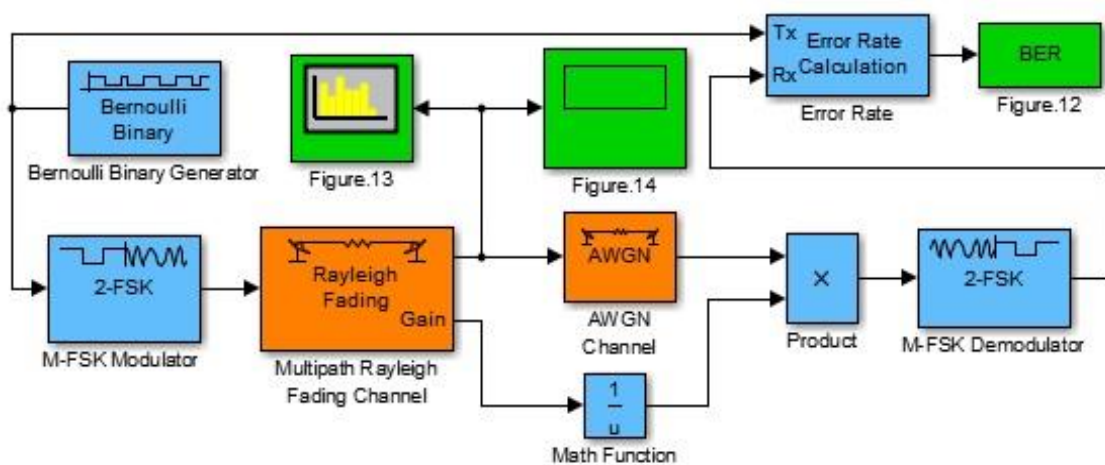


Figure 11. Simulink model of uncoded 2FSK under Rayleigh fading and AWGN channel

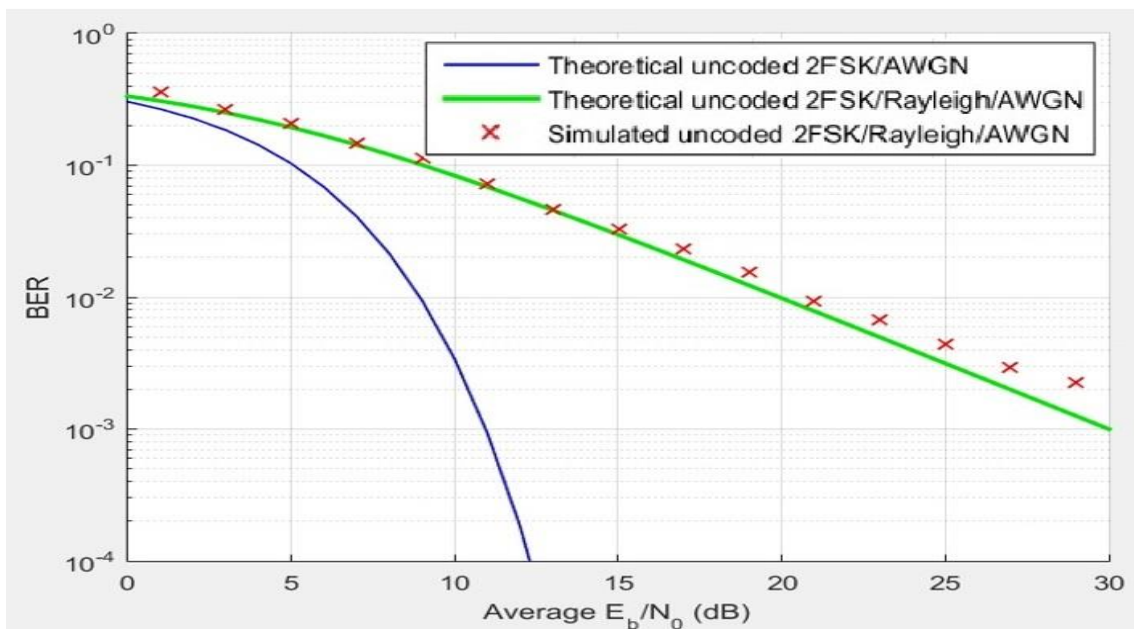


Figure 12. BER performance of non-coherent 2FSK under Rayleigh fading and AWGN channel

The degradation in BER performance is clearly noticeable in Fig.12. This is due to fading effect in the channel and hence some of coding process is required to enhance the

performance. The power spectral density of 2FSK at Rayleigh fading channel (using rectangular window and 1042 points FFT) can be shown in Fig.13 where two frequencies are located at 100 Hz and -100 Hz. Fig.14 shows the 10 sec time interval of Rayleigh output where the fading effect is clearly visible in the signal.

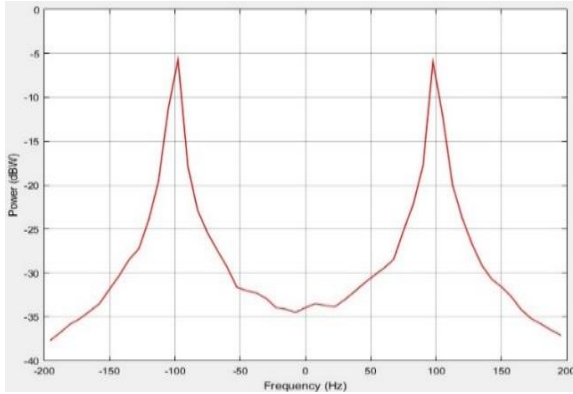


Figure 13. Power spectral density of uncoded 2FSK under Rayleigh fading effect

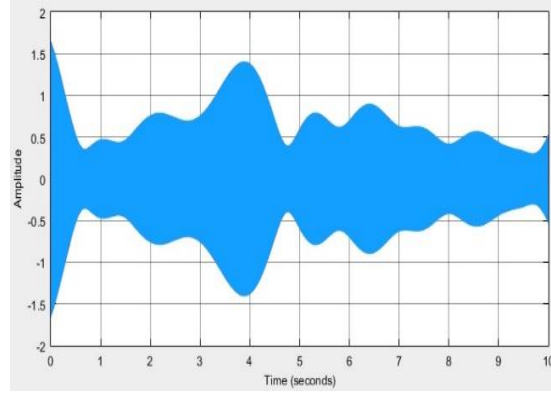


Figure 14. Rayleigh channel output for 10 sec time interval of uncoded 2FSK

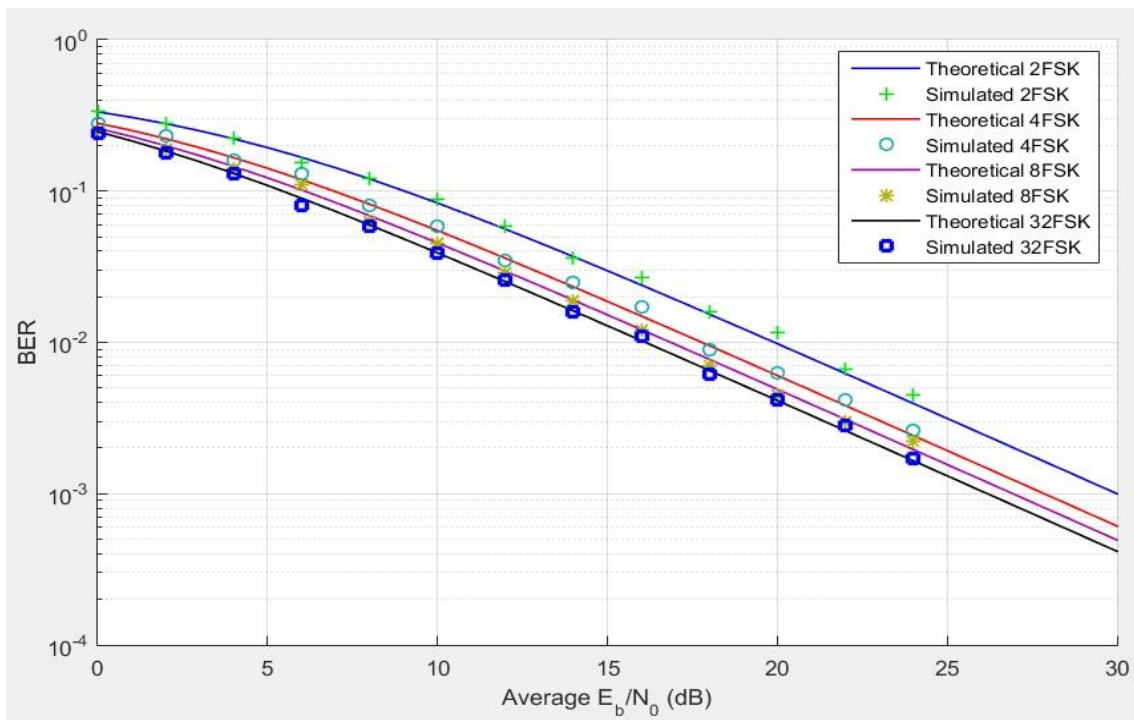


Figure 15. BER performance of non-coherent MFSK under Rayleigh fading and AWGN channel.

The theoretical and simulated BER performance for uncoded MFSK (M=2, 4, 8, and 32) under Rayleigh fading effect can be shown in Fig.15 where the theoretical performance is evaluated using (eq.7). Clearly there is an acceptable agreement that can be shown between the simulated and theoretical values.

To evaluate BER performance under Rician multipath fading, Fig.16 shows the Simulink model of coherent CPFSK (continues phase). The model parameters are modulation index=0.8, Jakes fading model [16] with Rice factor=three, maximum diffuse Doppler shift=0.2 Hz, paths delay= {zero, 2}, delay depth to compute BER is 16 sec, and average channels gain= {zero, X} dB, where X is the average gain of second path taking the values {-5, -10, -100} dB.

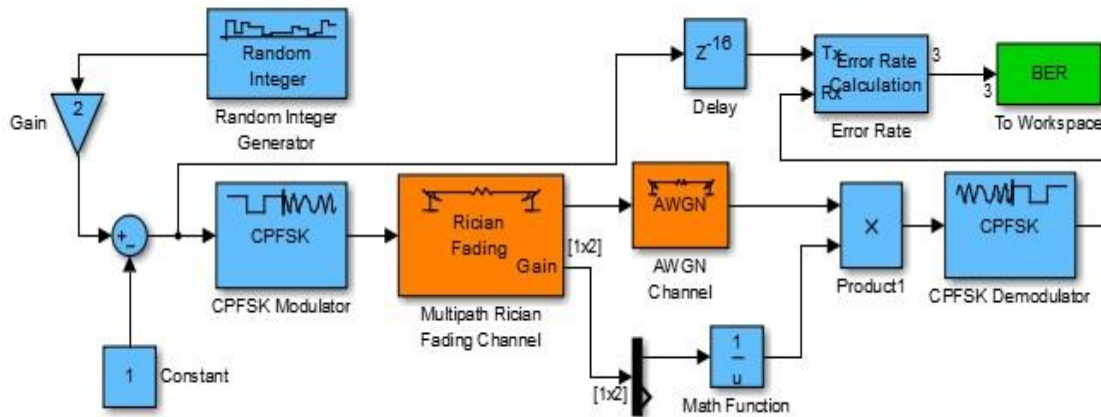


Figure 16. Simulink model of coherent CPFSK affected by Rician multipath fading (two paths)

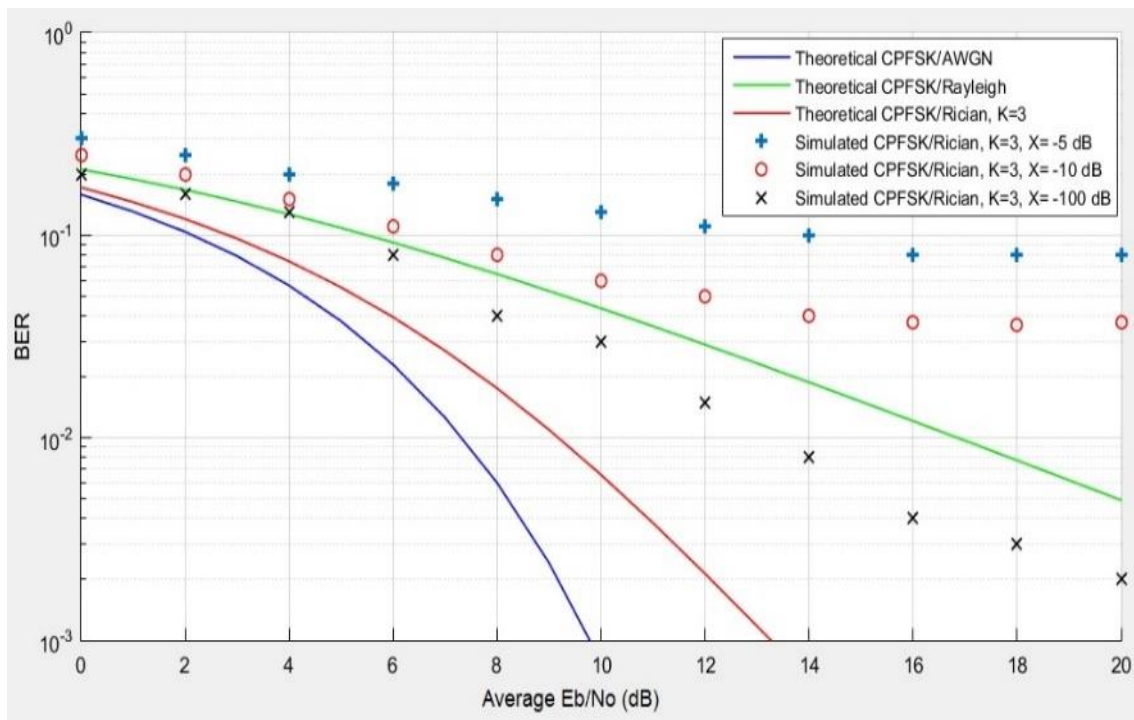


Figure 17. BER performance of coherent CPFSK under Rician multipath fading and AWGN channel

To follow the signal variation, the model uses the math function $1/u$ that acts as an automatic gain control by choosing the main path. Fig.17 shows the simulated BER performance under Rician multipath fading effect (2 paths) along with theoretical

performance (Rayleigh and Rician, $K=3$) of coherent FSK. Clearly, the BER performance is degraded even with weak multipath fading. So coding process is required to enhance the performance.

5.4 Coded MFSK under Rayleigh Fading Effect

To overcome the degradation in BER performance due to fading effect, 32FSK is combined with RS (31, 15) coder/decoder and 31x31 matrix interleaving. Fig.18 shows the Simulink model of coded 32FSK under Rayleigh fading effect with the following parameters: sample time=1 sec, symbol time=15/31 sec, 1000 samples per symbol, separation in frequency=100 Hz, interleaving and de-interleaving matrix size=31x31, the maximum Doppler shift is 0.1 Hz for Rayleigh Jakes fading model, gain factor to compute BER is 16/31, and delay depth to compute BER is 512 sec.

Fig.19 shows the simulated BER performance of coded 32FSK under Rayleigh fading effect along with theoretical uncoded 32FSK performance that is affected by AWGN and Rayleigh fading. The enhancement in BER performance (high coding gain) is clearly visible in the Fig due to using the combination of interleaving and RS (31, 15) coder/encoder under Rayleigh fading effect.

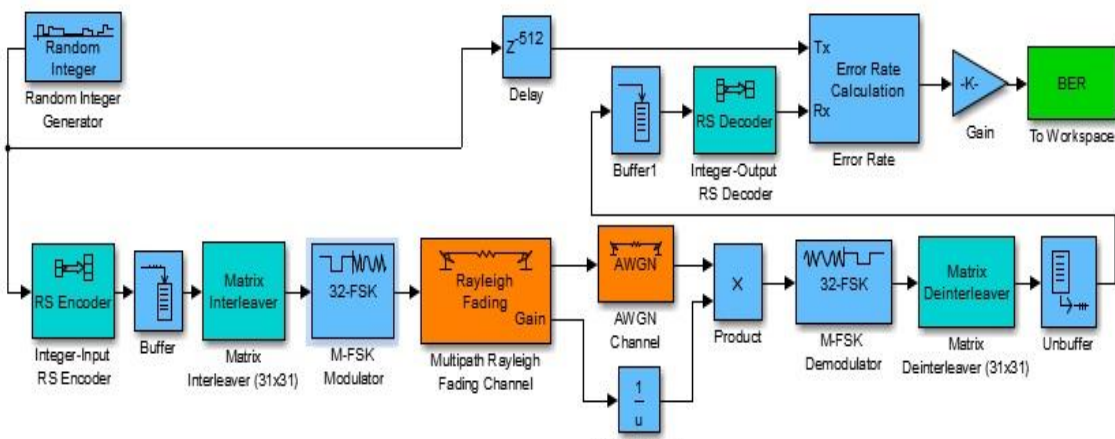


Figure 18. Simulink model of coded 32FSK with RS (31,15) and interleaving affected by Rayleigh fading

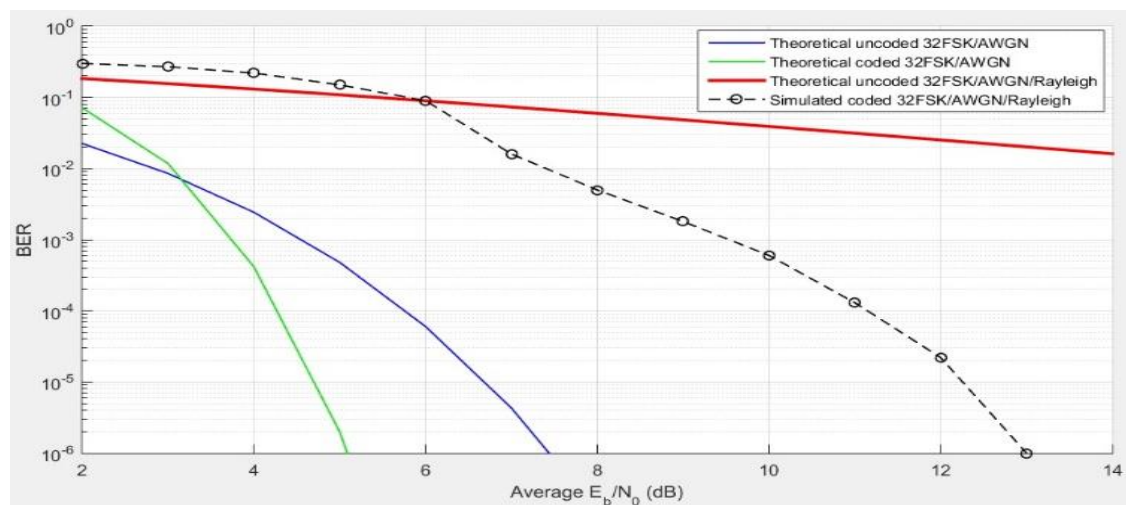


Figure 19. BER performance of coded 32FSK with interleaving and RS (31,15) under Rayleigh fading channel

5.5 Coded MFSK with STBC under Rayleigh Fading Effect

In wireless digital communications systems, usually STBC (multiple transmit and receive antennas) is used to compensate for low coding gain and to overcome the degradation in BER performance when such systems operate in fading environment. Fig.20 shows the Simulink model of coded 32FSK combined with 31x31 matrix interleaving, RS (31,15), and Alamouti (2x2) STBC [15,17]. This model uses two transmit paths and two receive paths with AWGN and four paths Rayleigh fading channel. The model parameters are: sample time=1 sec, symbol time=15/31 sec, 1000 samples per symbol, separation in frequency=100 Hz, interleaving and de-interleaving matrix size=31x31, the maximum Doppler shift is 0.1 Hz for four-path Rayleigh Jakes fading model in each path, gain factor to compute BER is 16/31, and delay depth to compute BER is 512 sec.

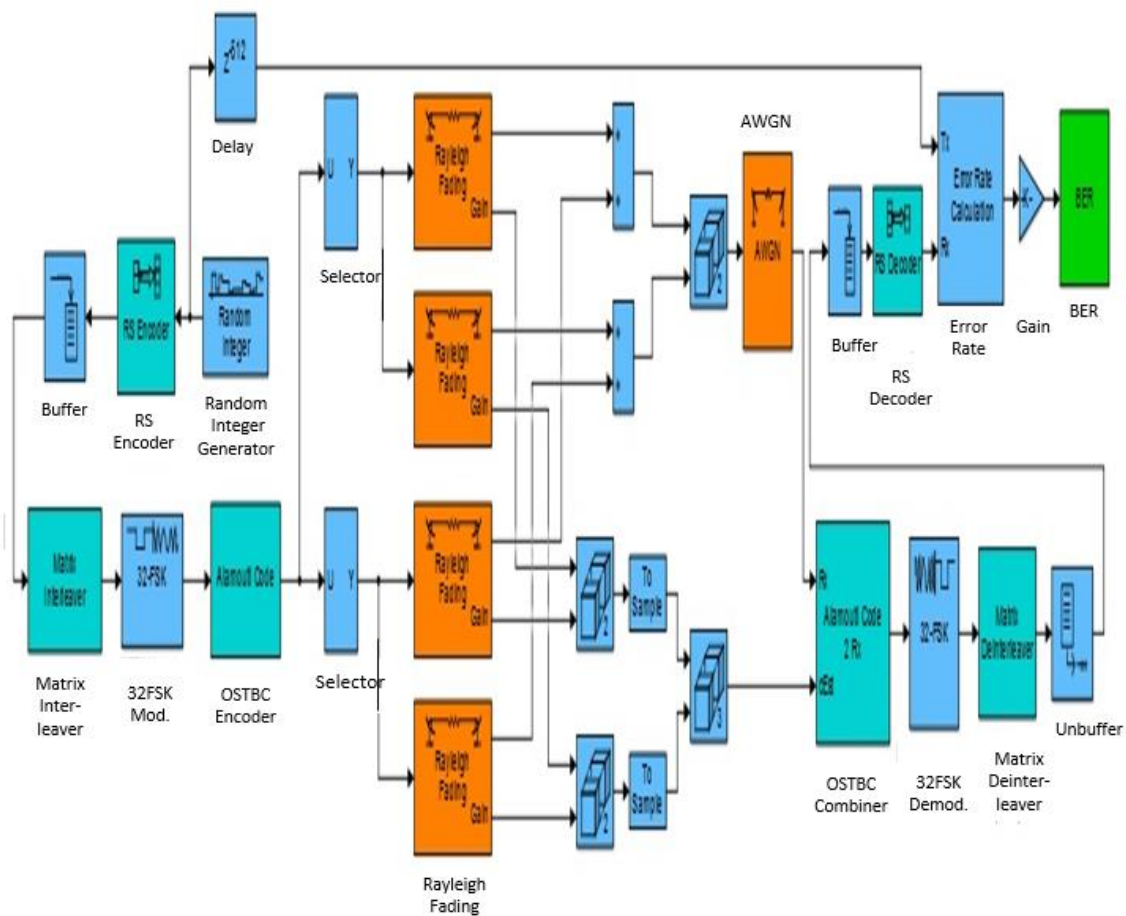


Figure 20. Simulink model of coded 32FSK with RS (31, 15), interleaving (31x31), and STBC (2x2) affected by Rayleigh fading channel

Fig.21 shows the BER performance of coded 32FSK when combined with (31x31) interleaving matrix size, RS (31, 15) coder/encoder, and Alamouti (2x2) STBC. This figure also shows the performance of uncoded 32FSK under Rayleigh fading effect with one and four diversity orders for comparison. The BER enhancement and high coding gain is clearly visible due to the combination of STBC with interleaving and RS coding.

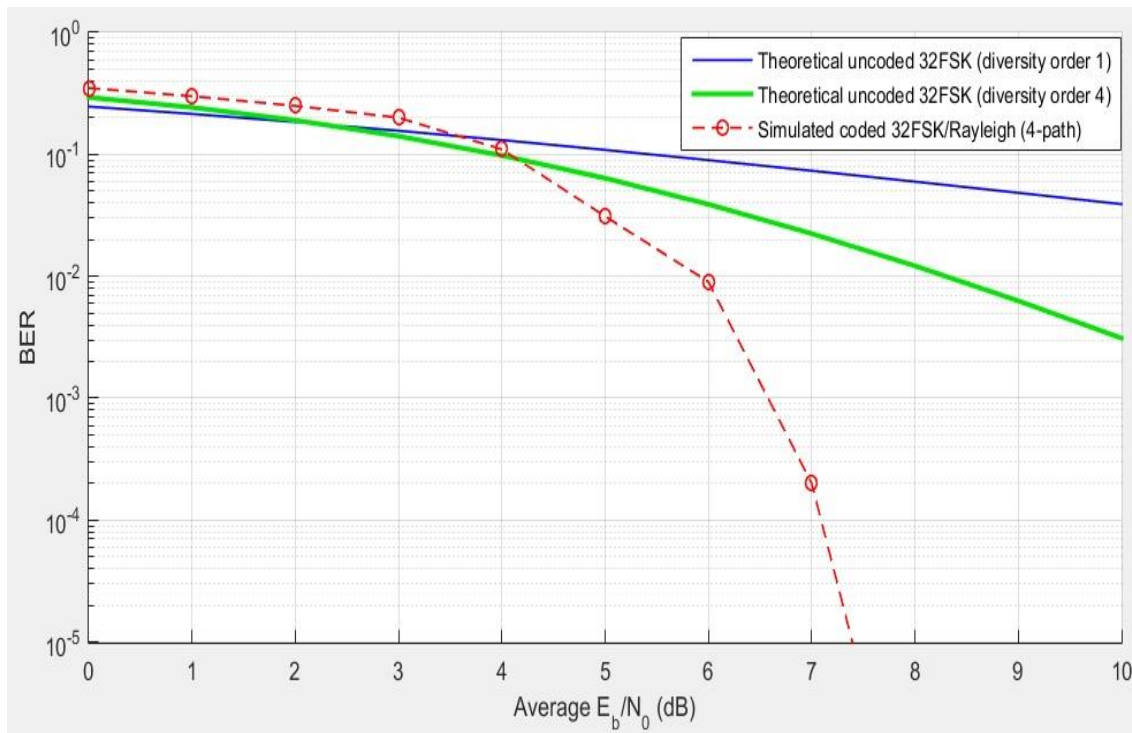


Figure 21. BER performance of coded 32FSK with interleaving (31x31), RS (31, 15), and STBC (2x2) under Rayleigh fading channel

6. Conclusions

This paper has analyzed the BER performance of MFSK modulation for several combinations of block codes and uncoded MFSK when these systems operate under AWGN and multipath fading environment (Rayleigh and Rician channels). Since the environment sets essential limits on the function of mobile communication structures, an error control and diversity scheme is required to compensate for BER degradation due to fading in received signal. For Rician multipath fading effect, BER performance is strictly degraded even with weak multipath (Fig.17 for $X=-100$ dB). From simulation results, it seems that Rayleigh fading effect caused the worst case in BER degradation. When combined the uncoded MFSK with interleaving and Reed Solomon coder/decoder, the enhancement in BER performance and hence high coding gain obtained is clearly noticeable in the Fig.19 due to using this combination of coding scheme. Additional enhancement in BER performance is gained by adding a space-time block coding (Alamouti STBC) to the combination of interleaving and RS coding (Fig.21). Using other coding scheme (such as Golay code) or high diversity order (rather than 2x2 that used in this paper) may give a significant high coding gain compared with uncoded MFSK model but at the expense of system complexity.

7. References

1. Proakis, J. G. and Salehi, M. (2007). "Digital Communications", 5th edition, McGraw-Hill.

2. Chandra, A. S. Poram, R. and Bose, C. (2008). "Performance of Coherent MFSK Schemes over Slow Flat Fading Channels", IEEE Region 10 Conference, TENCON, Hyderabad AP India, pp. 1-6.
3. Joshi, D. and Gupta K. (2012). "SEP performance of MFSK in Rician fading channel based on MGF method", IOSR Journal of Engineering, Vol. 2, No. 4, pp: 897-899.
4. Joshi, D. and Gupta K. (2012). "Performance Comparison between MPSK and MFSK in Rician Fading Channel based on MGF Method", International Journal of Computer Applications (0975 – 8887), Vol. 45, No.14, pp. 33-37.
5. Awon, N. T. Rahman, T. Islam, A. and Islam, T. (2012). "Effect of AWGN & Fading (Rayleigh & Rician) channels on BER performance of a WiMAX communication System", (IJCSIS) International Journal of Computer Science and Information Security, Vol. 10, No. 8, pp.11-17.
6. Babu, A. S. and Rao, K. V. (2011). "Evaluation of BER for AWGN, Rayleigh and Rician Fading Channels under Various Modulation Schemes", International Journal of Computer Applications (0975 – 8887) Vol. 26, No. 9, pp.23-28.
7. Chavan, M. S. Chile, R. H. and Sawant, S. R. (2011). "Multipath Fading Channel Modeling and Performance Comparison of Wireless Channel Models", International Journal of Electronics and Communication Engineering, (ISSN 0974-2166) Vol. 4, No. 2, pp. 189-203.
8. Michael, J. C. and Wayne, E. S. (2000). "Effect of Mobile Velocity on Communications in Fading Channels", IEEE transactions on vehicular technology, Vol. 49, No. 1, pp. 202-210.
9. Soni, M. Ghosh, P. K. and Gupta, K. (2015). "Review of Data Communication in Wireless Fading Channel and a Case Study", International Journal of Electronics & Communication Technology- India IJECT Vol. 6, Issue 1, pp. 49-55.
10. Oyetunji, S. A. and Akinninranye, A. A. (2013). "Comparing Performances of Bandpass Modulation in Wireless Communication Channels", Journal of Environmental Engineering and Technology Vol.2 No.2, pp. 25-34.
11. A. Goldsmith, "Wireless Communications", Cambridge University Press, 2005, Ch.8.
12. Ahmed, S. Yang, L. L. and Hanzo, L. (2007). "Erasure Insertion in RS-Coded SFH MFSK Subjected to Tone Jamming and Rayleigh Fading", IEEE Transactions on Vehicular Technology, Vol. 56, Issue 6, pp. 3563 – 3571.
13. Lie-Liang, Y. Kai, Y. and Hanzo, L. (2000). "A Reed-Solomon coded DS-CDMA system using noncoherent M-ary orthogonal modulation over multipath fading channels", IEEE Journal on Selected Areas in Communications, Vol. 18, Issue. 11, pp. 2240 – 2251.
14. Alamouti, S. M. (1998). "A simple transmit diversity technique for wireless communications", IEEE Journal on Selected Areas in Communications, Vol.16, Issue 8, pp.1451 – 1458.
15. Giordano, A. A. and Levesque A. H. (2015), "Modeling of Digital Communication Systems Using SIMULINK", published by John Wiley & Sons, Inc., Hoboken, New Jersey.
16. Mathworks Documentation, "Communications system toolbox", Matlab R2015a, <https://www.mathworks.com>.

17. Rahman M. and Sarkar S. (2016), "*Performance Estimation of Receiver for Variable MIMO-PSK Antenna Configurations with Alamouti Space Time Block Coding*", 5th International Conference on Computing, Communication and Sensor Network, Vol.2, Issue 5, pp. 80-85.